# Electrical and Mathematical Models of PV Cells: Strategies and Critical Assessment

**Marco Semeraro**
marco.semeraro26@gmail.com

**Instituto Superior Técnico, Universidade de Lisboa, Portugal**
**July 2020**

**Keywords:** PV Modelling, Parameter Extraction, Five-Parameter Model, Single-Diode Equivalent Circuit, I-V Curve

**ABSTRACT** - The main concerns with PV modelling are on the one hand, the number of degrees of freedom of the (most accurate) mathematical models with respect to the amount of available data and, on the other hand, their dependency on widely varying operating conditions. In this study, a framework for PV modelling is built with the aim to provide a tool for a rxeasoned selection of the modelling strategies, based on their physical implications. The diode-based models are analysed and the conventional techniques to extract their model parameters and account for their dependency on irradiance and temperature are presented along with their issues. The Complete Single-Diode Model featuring 5 model parameters proves to represent the best trade-off between simplicity and accuracy. For this reason, it is further analysed by comparing two different irradiance-temperature approaches, i.e. the Adaptive-Parameter Modelling (APM) and the Constant-Parameter Modelling (CPM). The parameter extraction based on the Newton-Raphson method proves to be a key step for the accuracy of both the models: when properly designed, it allows both the models to show excellent fit with the experimental data, whereas APM proves to perform slightly better than CPM at the expenses of the computing time.

## 1. Introduction

In science and engineering, a *model* is a representation (in various forms) of a phenomenon or system. A model facilitates the understanding of the system and provides a tool to simulate or predict its behaviour given certain conditions. When the phenomenon or system to be modelled is complex, a totally comprehensive representation of its functioning is often impossible; as a consequence, usually a model shows a certain level of simplification that is chosen with respect to the purposes it is built for. Both on research and industry level, effective mathematical PV modelling has gained crucial importance for different reasons and purposes: for engineers, to evaluate the economic feasibility of a PV system [1], select the most suitable module [2], check its status [3] and predict its performance under any weather condition [2]; for manufacturers, to optimize the fabrication process through the identification of the model parameters [4]; for researchers, to better understand the underlying physics through the proper interpretation of the model parameters. Additionally, PV modelling is crucial to design efficiently the power inverters [5] and the Maximum Power Point Trackers (MPPT) [6]. After all, it is well known that predictive performance tools such as models are an important factor in the success of any technology [1]. However, building a PV model that responds accurately and reasonably fast to varying irradiance G and cell temperature $T_c$ is not straightforward due to the non-trivial mathematical formulations that describe it. In general, if several experimental measurements can be carried out, the task is made much easier as the goodness of the model can be tuned and validated through real data fitting. However, on the industry-commercial level, performance data are available only for specific fixed environment conditions, i.e. the Standard Test Conditions (STC: G = 1000 $Wm^{-2}$, $T_c$ = 25 °C), making it harder to tune systems with multiple degrees-of-freedom such as PV models.

In the last decades, different theoretical approaches and numerical methods have been used to develop simulation models and parameters extraction techniques [6]. The aim of this work is to give a panoramic view on PV modelling with a novel structure: if the usual approach is pivoted around the *models* themselves, at the core of this work is the effort to provide an operative reference framework centred on the *strategies* (Section 2). In the light of the proposed framework, the models available in literature are then presented (Section 3) and compared (Section 4). Finally, to show the crucial importance of a careful choice of the modelling strategies, the most used model (5-parameter) is implemented, investigated (Section 5) and validated (Section 6).

## 2. PV Modelling Framework

A PV model consists of an *equivalent electrical circuit* represented by a *governing* (or *characteristic*) *equation,* expressed in terms of the current $I$ delivered by the PV device as a function of the voltage $V$ at its terminals; this function $I(V)$ produces a curve in the I-V plane, called *I-V curve*.

At the core of any semiconductor-based PV device is the so-called *p-n junction*, that on the one hand allows to collect the photo-generated current $I_{ph}$ and on the other hand behaves like a diode. A diode is described by the Shockley diode equation [7]:

$$I_d = I_s \left[ e^{\left(\frac{V_d}{aV_{th}}\right)} - 1 \right] \quad (1)$$

where:

- $I_d$ and $V_d$ are the current passing through the diode and the voltage at its terminals, respectively;
- $I_s$ is the *diode saturation current* and $a$ is the *diode ideality factor*;
- $V_{th}$ is the *thermal voltage*, defined as:

$$V_{th} = \frac{k_B T_d}{q} \tag{2}$$

where:

- $q$ is the electron charge (q = 1.602177·10$^{-19}$ C) and $k_B$ is the Boltzmann constant ($k_B$= 1.380649·10$^{-23}$ JK$^{-1}$);
- $T_d$ is the diode temperature.

From a strict physical point of view, the *p-n junction* of a PV device is represented by two diodes in parallel; however, on the one hand it can be represented also by a single diode and on the other hand, a third diode can be introduced to account for other phenomena. In the latter case, a Three-Diode Model (TDM) is obtained and it represents the most comprehensive PV model; its equivalent electrical circuit is shown in Figure 1. The series resistance $R_s$ and the parallel resistance $R_p$ account for a number of losses.

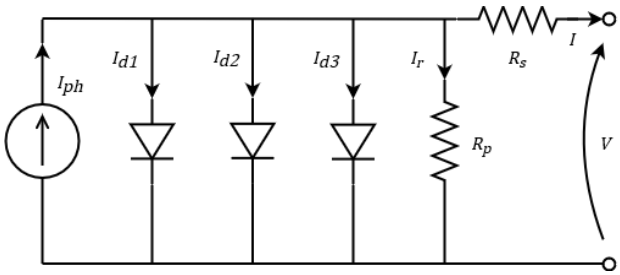


*Figure 1* Equivalent electrical circuit

Any simpler model is obtained from this one by neglecting one or more components, where the simplest model features just the current source and one diode (Ideal Single-Diode Model, ISDM). According to Kirchhoff Laws, the governing equation of the circuit shown in Figure 1 is:

$$I(V) = I_{ph} - \sum_{n=1}^{3} I_{sn}\left[e^{\left(\frac{V+IR_s}{a_n V_{th}}\right)} - 1\right] - \frac{V + IR_s}{R_p} \tag{3}$$

It is to be noted that, unless $R_s = 0$, this equation is in *implicit* form with respect to $I$. The corresponding I-V curve is shown in Figure 2 (the general features of an I-V curve are the same from the simplest to the most complex model): the three highlighted points are called *three remarkable points* (TRP) and are:

- the short-circuit point (SCP) $(0, I_{SC})$;
- the maximum power point (MPP) $(V_{MPP}, I_{MPP})$ in which the maximum power $P = VI$ is extracted from the device;
- the open-circuit point (OCP) $(V_{OC}, 0)$.

Equation (3) features a number of parameters (see Table 1) that depends on the components included in the equivalent circuit, from a minimum of 3 (ISDM) to a maximum of 9 (TDM). Of these, the ideality factor and the resistances deserve a closer analysis for their physical meaning and with respect to the features of the I-V curve.

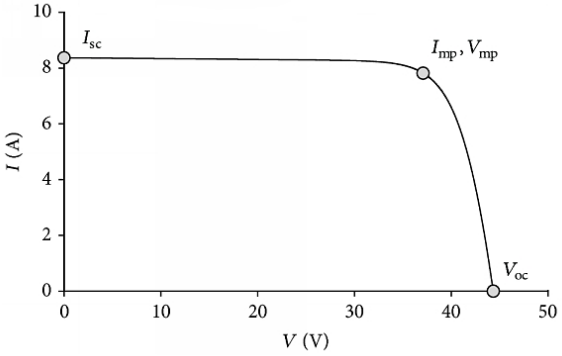


*Figure 2* General I-V curve

*Table 1* General parameters of a PV model

| Symbol | Description |
|---|---|
| $I_{ph}$ | photocurrent |
| $I_{sn}$ | saturation current of the n-th diode |
| $a_n$ | ideality factor of n-th diode |
| $R_s$ | lumped series resistance |
| $R_p$ | lumped parallel resistance |

*The ideality factor a*

It is characteristic of the semiconductor material of the PV device and the manufacturing process it undergoes [8]. The ideality factor is a measure of how closely the diode follows the ideal diode equation, defined for $a = 1$. Defects in the semiconductor are the main reason for $a$ to be higher than 1 [9], with values ranging from 1 at high currents up to 2 at low currents [10], but in some cases it can be even higher than 2 [4], especially for industrial cells [11]. When the chosen model features only one diode, usually $a$ lays in the range 1-1.5 [5]. On the I-V curve (Figure 3), the value of the ideality factor affects the knee shape around the MPP ("curvature" of the I-V curve). The ideality factor is usually used as adjustment parameter to improve the accuracy of the model [5, 1], even though an estimation that is independent from the curve fitting is desirable [2].

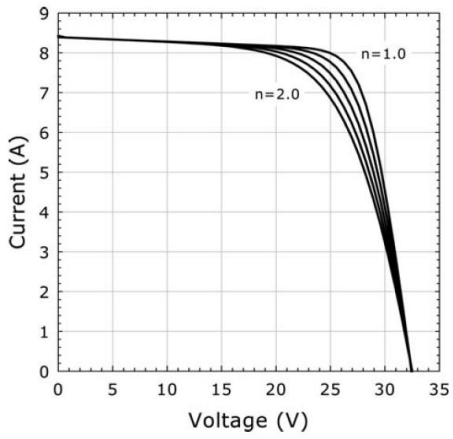


*Figure 3* Influence of $a$ ("n") on the I-V curve [9]

*The series resistance $R_s$ and the parallel resistance $R_p$*

It is worth highlighting that both the series and parallel resistances do not physically exist [1] as they are *lumped* circuit components accounting for phenomena occurring

diffusely throughout the cell. $R_s$ accounts for the resistivity of [5, 6] the semiconductor material that is not heavily doped, of the metal grid, of the contacts and of the current-collecting wires. Usually it is lower than 1Ω [12]. $R_s$ is related to the slope of the I-V curve at open-circuit condition. $R_p$ accounts for the unavoidable series of shunts (i.e. high-conductivity paths) forming throughout the large area of semiconductor material that constitutes a PV cell [5, 6]; the order of magnitude of its value goes from 10 up to $10^3\,\Omega$ [12]. $R_p$ is related to the slope of the I-V curve at short-circuit condition. Both $R_s$ and $R_p$ give an indication of the quality of the semiconductor material, in fact often they are used as manufacturing check and test [5, 13].

### 2.1 Parameter Extraction Methods

In order to use a model for simulations or predictions, the model must be mathematically defined, meaning that all the unknown parameters must be identified. This process is called "parameter extraction" (or identification) and it is crucial since all studies agree that the accuracy of any PV cell model depends mainly on the accuracy of the extracted model parameters [8]. For instance, all the components in the equivalent circuit should be physically realistic, (e.g. a resistance cannot have a negative value). From a mathematical point of view, identifying $n$ unknown parameters means setting $n$ analytically-independent equations [3, 14]. These equations are mainly derived imposing the matching of the modelled I-V curve with the experimental one. However, as usually only a limited set of information is commercially-available, a *limited* number of constraints can be set. As a result, for the models of main interest, i.e. those with a medium-high level of complexity, the solving system of equations is *dependent*. In these cases, *iterative* numerical methods and weighted initial guesses on parameters are employed to search for (only) an approximated solution of the model parameters.

The information provided on the module datasheet include the coordinates of the TRP at STC therefore, a maximum of *four constraints* can be set:

1) matching at the SCP: $I(0) = I_{SC}$ ;
2) matching at the OCP: $I(V_{OC}) = 0$ ;
3) matching at the MPP: $I(V_{MPP}) = I_{MPP}$ ;
4) modelled MPP actual maximum of the power function:

$$\left.\frac{dP}{dV}\right|_{V=V_{MPP}} = 0 \qquad (4)$$

Usually, these equations are written in the normal form $f_i(\boldsymbol{X}) = 0$, where $\boldsymbol{X}$ is the vector of the unknowns, i.e. the model parameters. Any system of equations derived from the aforementioned constraints is (*cf.* Equation (1)) 1) *nonlinear,* due to the presence of one or more exponential terms and 2) *implicit,* since so are the equations. For these reasons, numerical methods are used to solve these systems; the most used are [3, 15] the Newton-Raphson method (NR), a manual trial-and-error routine and the Bisection method. They need an initial guess of the parameters and they might not converge at all if the initial guesses are too far from the actual solutions [16, 15].

When the chosen model has more than 4 parameters, a strategy must be adopted; the main options are:

1) reducing the number of parameters by making weighted assumptions (common in models with several parameters);
2) finding an approximated solution by iterating on initial guesses (common in five-parameter models);
3) setting additional I-V constraints based on the graphical interpretation of the resistances.

Clearly, a mix of the above is also possible. Sometimes, simplifications are introduced in order to make equations more manageable. The two most common simplifications are $I_{ph} \sim I_{SC}$ and neglecting the "-1" in the Shockley diode equation at OCP.

### 2.2 Dependence on Irradiance and Temperature

A single I-V curve and its $I(V)$ equation represent the behaviour of a PV device only for well-defined operating conditions, i.e. irradiance $G$ and cell temperature $T$. However, during normal operation, these conditions vary significantly.

As regards irradiance, the main contribution is given by the photocurrent as the more the irradiance, the more the light-generated current; as the irradiance decreases the curve shifts downwards to lower values of $I_{SC}$. Consequently, also the (maximum) power delivered and the general performance degrade. Voltage is generally less affected by variations in irradiance.

As regards the (cell) temperature $T_c$, as it increases, the open-circuit voltage decreases more than the short-circuit increases, leading to a decrease of $P_{MPP}$ and an overall deterioration of the performance. The reason behind this behaviour lies in the reduction of the bandgap energy of the semiconductor.

Mainly, there are two kind of formulations that allow to evaluate the $(G, T_c)$-dependence of the model:

- *theoretical* equations derived from the physics;
- *experimental* expressions that use experimental coefficients provided by the manufacturers, i.e. the *temperature coefficients* $(\alpha_T, \beta_T, \gamma_T\ \delta_T, \omega_T)$; in this case the irradiance is considered to affect only the short-circuit current (or the photocurrent).

A mix of the two approaches is also possible. In the following, the subscript "$ref$" indicates known quantities; usually these are the STC values.

<u>*Dependence of the TRP*</u>

The short-circuit current varies according to [3, 5]:

$$I_{SC}(G, T_c) = \frac{G}{G_{ref}} I_{SC,ref}\left[1 + \alpha_T\left(T_c - T_{c,ref}\right)\right] \qquad (5)$$

As regards the MPP, usually the temperature coefficient on $P_{MPP}$ is provided but those on $I_{MPP}$ and $V_{MPP}$ are rarely found:

$$P_{MPP}(T_c) = P_{MPP,ref}\left[1 + \gamma_T\left(T_c - T_{c,ref}\right)\right] \qquad (6)$$

$$I_{MPP}(T_c) = I_{MPP,ref}\left[1 + \delta_T\left(T_c - T_{c,ref}\right)\right] \qquad (7)$$

$$V_{MPP}(T_c) = V_{MPP,ref}\left[1 + \omega_T\left(T_c - T_{c,ref}\right)\right] \qquad (8)$$

The open-circuit voltage can be updated with (experimental):

$$V_{OC}(T_c) = V_{OC,ref}\left[1 + \beta_T\left(T_c - T_{c,ref}\right)\right] \quad (9)$$

or (theoretical):

$$V_{OC}(T_c) = V_{OC,ref}\left(\frac{T_c}{T_{c,ref}}\right) + E_g\left(1 - \frac{T_c}{T_{c,ref}}\right) \quad (10)$$

and:

$$V_{OC}(G) = V_{OC,ref} + aV_{th}ln\left(\frac{G}{G_{ref}}\right) \quad (11)$$

where $E_g$ is the energy bandgap of the semiconductor.

*Dependence of the model parameters*

As $I_{ph} \sim I_{SC}$, the photocurrent can updated with:

$$I_{ph}(G, T_c) = \frac{G}{G_{ref}} I_{ph,ref}\left[1 + \alpha_T\left(T_c - T_{c,ref}\right)\right] \quad (12)$$

The saturation current can be evaluated from the characteristic equation at OCP with (experimental):

$$I_s(G, T_c) = \frac{I_{ph}(G, T_c) - \frac{V_{OC}(G, T_c)}{R_p}}{e^{\left[\frac{V_{OC}(G,T_c)}{aV_{th}}\right]} - 1} \quad (13)$$

or, alternatively, with (theoretical):

$$I_s(T_c) = I_{s,ref}\left(\frac{T_c}{T_{c,ref}}\right)^3 e^{\frac{qE_g}{ak_B}\left(\frac{1}{T_{c,ref}} - \frac{1}{T_c}\right)} \quad (14)$$

Usually, the ideality factor(s) of the diode(s) and the resistances are considered constant [17] (*Constant-Parameter Modelling*, CPM). In reality, they do vary and neglecting their variations might lead to model errors [18] (*Adaptive-Parameter Modelling*, APM). However, explicit expressions for the dependency of $R_s$, $R_p$ and $a$ on temperature and irradiance are not used; rather, they are extracted for every pair of irradiance and temperature.

The correlations herein presented need to be accounted for in the model equation; two main approaches can be followed, according to the amount of available data:

1) extract the parameters at STC and then update their values separately; this is the most common approach since it relies on the information given by manufacturers; the choice of which parameters to consider and which law to use to update them is up to the author and his/her *ad hoc* considerations [3, 1]; often these correlations are used already in the parameter extraction step;
2) perform a parameter extraction for various pairs of temperature and irradiance in order to extract an expression $f_i(G, T)$ for each parameter through curve fitting; this method is less used as the temperature coefficients for MPP are often missing.

### 2.3 Model Validation and Performance Indices

A *good* PV model is a model that is able to fit at most the real (experimental) I-V curve under any environmental conditions. Different performance-evaluating methods can be found in literature and the choice of which of these is more appropriate depends on the specific purpose of the modelling. The most relevant are:

- Root-Mean-Square Deviation (RMSD) on the currents:

$$RMSD_I = \sqrt{\frac{\sum_j^N \left(\widetilde{I_j} - I_j\right)^2}{N}} \quad (15)$$

  where the tilde marks the points computed from the model versus the $N$ experimental values. If it is normalized to $I_{SC}$, it is called *Normalized RMSD* (NRMSD) and it is expressed in %. A RMSD and NRMSD (reference: $P_{MPP}$) for the power curve can be defined analogously;
- absolute and relative (with respect to the measured value) errors on each of the TRP; for example, for $I_{SC}$:

$$\varepsilon = \widetilde{I_{SC}} - I_{SC} \qquad \varepsilon_{\%} = \frac{\varepsilon}{I_{SC}} \quad (16)$$

## 3. PV Models

As already introduced in Section 2, a criterion to categorize the available PV models is the number of diodes present in the equivalent circuit (from 1 to 3): Table 2 summarizes the physical meaning of each diode along with the typical value of its ideality factor; if only one diode is present, usually $a \in [1, 1.5]$. An alternative and almost equivalent classification takes the number of the parameters featured in the $I(V)$ equation [6]: 3-parameter, 4-parameter, 5-parameter, 7-parameter and 9-parameter models.

*Table 2* Physical meaning of the model diodes

| Diode | Represented Phenomena | $a$ |
|---|---|---|
| $D_1$ | diffusion (and recombination in the quasi-neutral regions) | 1 |
| $D_2$ | recombination in the space-charge regions | 2 |
| $D_3$ | recombination in the defect regions, grain boundaries, etc | >2 |

With reference to Figure 1 and Equation (3), if only a current source in parallel with a diode is considered, the simplest model is obtained, i.e. the Ideal Single-Diode Model (ISDM) featuring 3 parameters. if a resistance is added to ISDM, a "Simplified Single-Diode Model" (SSDM, 4 parameters) is obtained while if both are used a "Complete Single-Diode Model" (CSDM, 5 parameters) is built. If both the resistances are allowed in the model, a further step up in the diode complexity is then justifiable: adding a second diode in CSDM one obtains the "Double-Diode Model" (DDM, 7 parameters) and if a third diode is added, a "Three-Diode Model" (TDM, 9 parameters) is obtained. The governing equation of the each model is obtained from Equation (3) by neglecting the corresponding parameters of the absent components (e.g. $R_s = 0$ if the series resistance is not present and $R_p \to \infty$ if the parallel resistance is missing). Then, the model can be developed according to the strategies presented in the framework in Section 2.

## 4. Model Comparison

*About the Number of Diodes*

When evaluating the number of diodes, CSDM is to be taken as reference for the single-diode models as it features both the resistances like its "contestants", DDM and TDM. First of all, CSDM proves to be the most widely model used choice to simulate PV power systems as it offers the most reasonable trade-off between simplicity and accuracy [3, 5, 8, 6]. However, the single-diode models assume that the recombination losses in the depletion region are negligible if not completely absent, while in a real PV cell these losses can be significant [19]. This difference does not emerge at STC; however, at low irradiance (during shading) DDM delivers significantly more accurate results than CSDM, especially in the proximity of $V_{OC}$ [7, 16]. In general, DDM seems to show less sensitivity to irradiance when compared to CSDM.

TDM seems to relate to DDM in the same way DDM relates to CSDM that is, the third diode improves the accuracy and the sensitivity to variations in the operating conditions. This is especially marked and useful when modelling relatively complicated materials such as polycrystalline silicon cells [3, 20, 6, 15] and when dealing with small size PV cells (research), since these cells are affected by greater leakage current through peripheries [21]. On the other hand, DDM and TDM are very sensitive to the initial conditions and this can lead to inconsistent results if not properly guided by an initial estimate of the parameters [1].

*About the Dependence on Temperature and Irradiance*

Of particular interest is the strategy to account for irradiance and temperature variations. In this sense, the Adaptive-Parameter Modelling (APM) has proved to be superior with respect to Constant-Parameter Modelling (CPM) both on the theoretical and practical level. In fact, assuming a number of parameters to be independent from the operating conditions is widely accepted as a simplification that does not reproduce the reality.

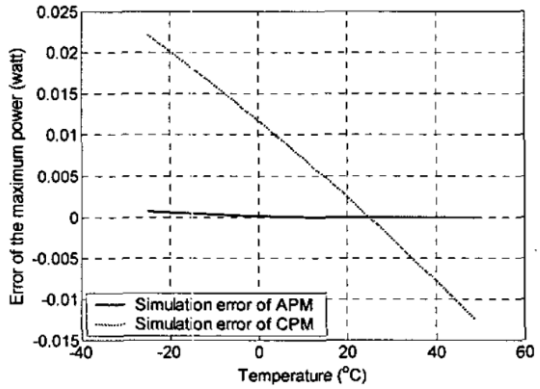


*Figure 4* Comparison between APM and CPM [18]

A proof comes from the results obtained in [18] for SSDM-s (see Figure 4) where APM shows constant (null) error with respect to temperature while CPM shows a trend. Nevertheless, it must be noted that only a 0.03 W error gap on 40 W is found over a 60°C range in CPM: in this case, the evaluation of the computing time of the two approaches is essential for an exhaustive and meaningful comparison as APM is much more time-consuming than CPM (model parameters have to be re-computed for every irradiance and temperature).

## 5. Proposed Models and Methodology

In this study, the Complete Single-Diode Model (CSDM) featuring 5 parameters is investigated. This model has been chosen because, despite the wide literature available on it, poor reference is found on the different strategies to account for varying operating conditions for this model. In this study, a CSDM with Adaptive-Parameter Modelling (APM) and a CSDM with Constant-Parameter Modelling (CPM) are implemented, investigated and compared. Moreover, a study on the effect of the parameter initial guesses on the parameter extraction performance is conducted. The proposed models make use only of the datasheet information.

The $I(V)$ equation for CSDM is:

$$I = I_{ph} - I_s\left[e^{\left(\frac{V+IR_s}{aV_{th}}\right)} - 1\right] - \frac{V + IR_s}{R_p} \qquad (17)$$

In the APM version of the model, the TRP are computed for the given cell temperature $T$ and irradiance $G$ according to Equations (5)-(9). Once the TRP are updated, a parameter extraction is performed for the given pair $(G, T_c)$ so that *all* model parameters are *adapted* to the operating conditions.

In the CPM version of the model, a preliminary one-timer parameter extraction is performed at STC. The obtained model parameters are used as reference to build the model's response to any irradiance and any temperature; the photocurrent $I_{ph}$ is updated through Equation (12) while the saturation current $I_s$ is updated with Equation (14).

For both APM and CPM, the irradiance is assumed to affect only the photocurrent. In CPM, it is assumed that the ideality factor and the resistances are constant with respect to both the irradiance and the temperature

### 5.1 Parameter Extraction Algorithm

The models are implemented in a Python script. The solving constraints (4) are applied to Equation (17) and set without any simplification. The function `fsolve` (SciPy package) finds their solutions applying the Newton-Raphson method on the corresponding functions, i.e. the four solving equations are set in the form:

$$\begin{cases} f_1(\boldsymbol{X}) = 0 \\ f_2(\boldsymbol{X}) = 0 \\ f_3(\boldsymbol{X}) = 0 \\ f_4(\boldsymbol{X}) = 0 \end{cases} \qquad (18)$$

where $\boldsymbol{X}$ is the vector of the unknown model parameters. Since the `fsolve` function runs only when an *independent* system is fed to it (i.e. a number of equations equal to the number of unknowns), one out of the 5 parameters must be set fixed: the ideality factor has been chosen as fixed parameter (therefore, $\boldsymbol{X} = [I_{ph}, I_s, R_s, R_p]$) because of the limited range of values that it proved to assume according to the reviewed literature. In fact, as this range is limited, the ideality factor can still be evaluated through an iteration loop. The `fsolve` function tries to find the solution vector

$\boldsymbol{X}_{sol}$ that minimizes the residuals of system (18). In order to do this, it needs an initial guess for each of the unknowns and this is crucial for the accuracy of the performance and for the execution time. If the initial guesses are too far from the actual solution, the algorithm diverges and fails, returning no solution. For this reason, an evaluation of the initial guesses has been conducted as follows:

- $I_{ph} = I_{SC}$
- $I_s$ is evaluated through Equation (13) for every $a$ ($R_p \to \infty$)
- $R_p$ is evaluated as: $R_p = \frac{V_{MPP}}{I_{SC} - I_{MPP}} - \frac{V_{OC} - V_{MPP}}{I_{MPP}}$
- $R_s$ is set to zero.

At the beginning, the loop on $a$ was set in the range [1.0, 2.0] with 0.01 steps. The performance index of the extraction over the $a$-loop was chosen to be the RMSD on the residuals of system (18), as natural extension of the NR-based `fsolve` algorithm itself. The RMSD is used as selection criterion to choose between the various solutions, meaning that the selected solutions ($a_{sol}, \boldsymbol{X}_{sol}$) are those for which RMSD is minimum. Also, a physical-consistency constraint is set on the solutions, i.e. that all of the parameters must be non-negative.

After various trials, $a_{sol}$ showed to lie always below 1.55, which is consistent with the results obtained from other authors, who indicated $a$ to lie in the range [0, 1.5]. For this reason, the loop on the ideality factor was reset to [1.0, 1.55] as looping showed to be the main time-consuming factor. During manual trials, another factor seemed to impact the extraction results, i.e. the initial guess on the series resistance. For this reason, a second loop on $R_{s,in}$ was set outer of the loop on $a$, in the range [0, 0.15] with 0.01 steps. It is worth to note that while the loop on $a$ sets a *fixed* model parameter, the loop on $R_s$ sets "only" its *initial* guess $R_{s,in}$.

A performance analysis was conducted and partial results are shown in Figure 5. A first clear result is the confirmation that for $a > 1.55$ the performance drops significantly. The loop-nested selection criterion on minimum RMSD picked as best solution the pair ($a = 1.52$, $R_{s,in} = 0.13$); however, from the picture it is clear that other solutions give a similar RMSD but are discarded as they perform slightly worse.

In fact, the following can be noticed:

- there is a solution convergence around $a = 1.52$ where the gaps between the RMSD are minimal (and in the domain of $10^{-16}$!);
- this convergence zone is dangerously close to the divergence zone, i.e. the abovementioned $a > 1.55$, meaning that on the one hand, a slightly too conservative upper boundary on the $a$-loop could cut out the best solutions and on the other hand, a too loose upper boundary would be inefficient time-wise;

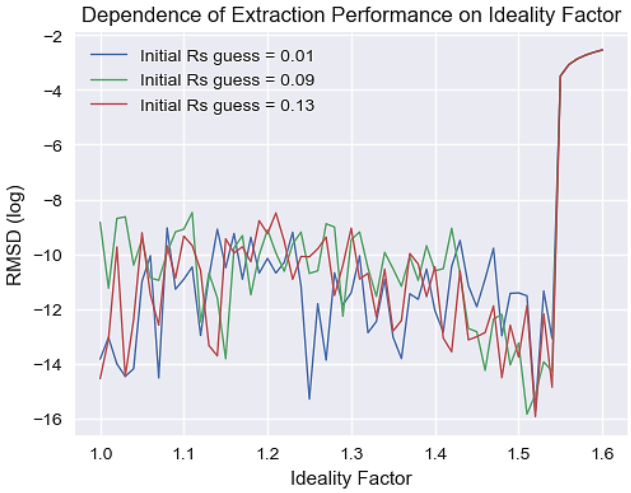


*Figure 5* Dependence of $log_{10}(RMSD)$ on $a$ for different $R_{s,in}$

- overall, the plots show similar trends apart from a couple of zones, that are [1.00, 1.05] and 1.25, where $R_{s,in} = 0.09$ shows an interesting valley;
- other two areas of accumulation for possible solutions appear in the range [1.0, 1.1] (except for $R_{s,in} = 0.09$) and around 1.15: here, if on the one hand the RMSD is about two orders of magnitude higher than the selected solution, on the other hand it is still extremely low ($\sim 10^{-14}$) and it "appears" significantly earlier in the $a$-loop (i.e. faster execution time).

These considerations suggested that the best fit on the constraint equations (that is, the best match at TRP and the MPP as actual maximum of the power curve), RMSD, might not be a truthful criterion on its own. From a mathematical point of view, this is expectable as the system is dependent. Even if a a fifth equation can be simulated by setting a loop on one of the unknowns (herein it was chosen $a$, but can be any of the others), a *real* fifth piece of information is still missing. This means that the *numerical best* fit on the TRP might not be the actual best fit on the real PV device. This will emerge clearly in the simulations presented in Section 6.

A further level of analysis can be carried out with respect to the computing time of the parameter extraction algorithm. Figure 6 shows its dependence on the upper boundaries for the $a$-loop and the $R_{s,in}$-loop: the influence of each upper limit is evaluated setting the other at its lowest in order to reduce the mutual influence. $R_{s,in,max}$ appears to have a nonlinear influence and stronger than that of $a_{max}$, which appears to be almost constant. When they are set both on higher values, the behaviour appears to be a superimposition of the separate trends: as a reference, for $a_{max} = 1.2$ and $R_{s,in,max} = 0.1$ the computing time is around 500 ms while for $a_{max} = 1.55$ and $R_{s,in,max} = 0.15$ it jumps to 900 ms. The reason might lie in the trial-and-error structure of the `fsolve` function.

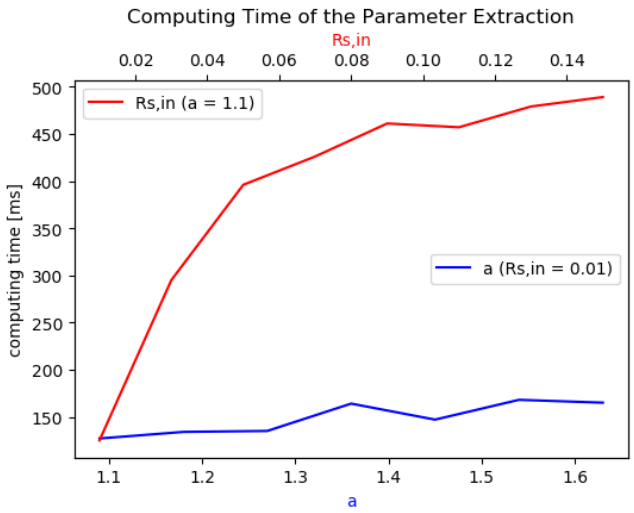


*Figure 6* Computing time as function of the loops upper boundaries

Finally, either the chosen model is APM or CPM, a careful design and a preliminary evaluation of the extraction process is herein suggested in order to highlight behaviours that are specific to the module and the solving algorithm, so to optimize the results and the extraction process itself.

Figure 7 shows the algorithm of the implemented code. The *effective irradiance* $G_{eff}$ is computed according to the model presented in [7] in order to account for the influence of the *angle of incidence* and of the *dirt* on the module. The model uses the measured values of POA irradiance ($G_T$), Direct Normal Irradiance (DNI), Diffuse Horizontal Irradiance (DHI) and the date and time to compute the angle of incidence (knowing the mounting angles: azimuth α, slope β, etc). The code features a degree of parameterization as it allows to sweep within the uncertainty range on irradiance and temperature, set the degree of dirtiness of the module and choose the upper limit on the $a$-loop, $a_{max}$.

## 6. Evaluation of the Proposed Models

The proposed models are tested and evaluated by comparison of their results with experimental data. The experimental data to validate the models has been taken from the publicly available database of the NREL [22]: the datasheet data is shown in Table 3 and the mounting details in Table 4.

A preliminary parameter extraction is carried out at STC to initialize CPM. Since the measurements were executed in a laboratory, the dirtiness is neglected. Given the doubts emerged in Section 5, the upper loop boundaries $R_{s,in,max}$ and $a_{max}$ were explored in different combinations. The results of the parameter extractions are shown in Table 5.

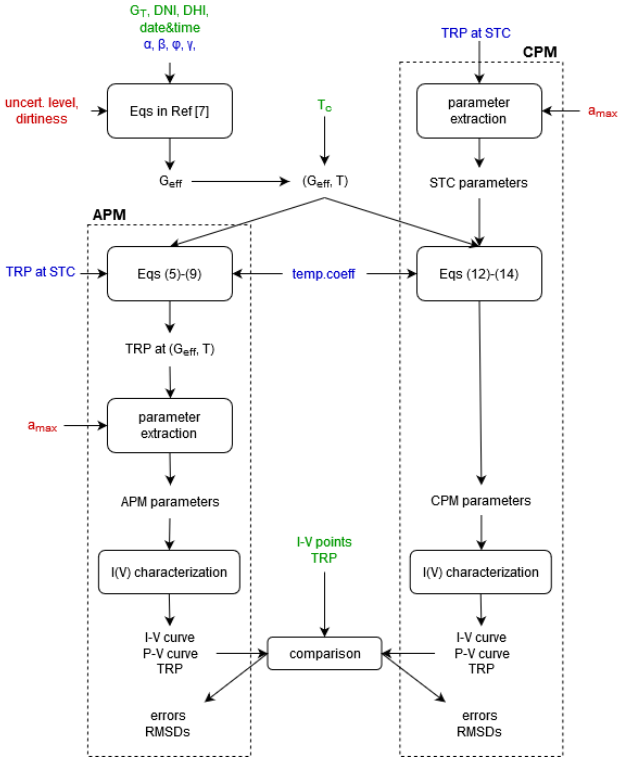


*Figure 7* Flowchart of the implemented code: blue quantities are taken from the datasheet, green ones from the measured dataset and red one are user's inputs

*Table 3* Datasheet values for the tested mono-Si module

| Quantity | Symbol | Value | Unit |
|---|---|---|---|
| Short-Circuit Current | $I_{SC}$ | 5.127 | A |
| Open-Circuit Voltage | $V_{OC}$ | 22.06 | V |
| Voltage at MPP | $V_{MPP}$ | 17.58 | V |
| Current at MPP | $I_{MPP}$ | 4.724 | A |
| Power at MPP | $P_{MPP}$ | 83.04 | W |
| Temp. Coefficient on $I_{SC}$ | $\alpha_T$ | 0.05 | %/°C |
| Temp. Coefficient on $V_{OC}$ | $\beta_T$ | -0.34 | %/°C |
| Temp. Coefficient on $I_{MPP}$ | $\delta_T$ | 0.01 | %/°C |
| Temp. Coefficient on $V_{MPP}$ | $\varepsilon_T$ | -0.43 | %/°C |
| Temp. Coefficient on $P_{MPP}$ | $\gamma_T$ | -0.42 | %/°C |

*Table 4* Mounting detalis

| Quantity | Symbol | Value | Unit |
|---|---|---|---|
| Azimuth | $\alpha$ | 0 | ° |
| Slope (Tilt) | $\beta$ | 28.5 | ° |
| Latitude | $\varphi$ | 28.39 | ° |
| Longitude | $\lambda$ | -80.46 | ° |
| Timezone | $ET$ | UTC-5 (-4 in DST) | |

As expected, the solutions appear to converge around two sets of values depending on $a_{max}$: one with $a = 1.52$ and the other with $a = 1.14$, where the former features higher $I_s$ and $R_p$ and lower $R_s$ than the latter. These differences are visible in the I-V curves produced by the two sets (see Figure 8) at STC. However, as expected, the errors on the TRP are *exactly the same* if the physical quantities are considered with a precision of $10^{-4}$ (the RMSD of the extraction for the two sets is in the orders of $10^{-14}$ - $10^{-16}$!).

*Table 5* Parameter extraction results

| $R_{s,in,max}$ | $a_{max}$ | comp. time [ms] | Iph [A] | Is [A] | a | Rs [Ω] | Rp [Ω] |
|---|---|---|---|---|---|---|---|
| 0.05 | 1.2 | 285 | 5.139 | 1.03e-09 | 1.07 | 0.35 | 150 |
| 0.10 | 1.2 | 365 | 5.136 | 4.07e-09 | 1.14 | 0.32 | 177 |
| 0.15 | 1.2 | 420 | 5.136 | 4.07e-09 | 1.14 | 0.32 | 177 |
| 0.05 | 1.55 | 415 | 5.127 | 7.79e-07 | 1.52 | 0.19 | 3023 |
| 0.10 | 1.55 | 590 | 5.127 | 7.01e-07 | 1.51 | 0.19 | 2129 |
| 0.15 | 1.55 | 749 | 5.127 | 7.79e-07 | 1.52 | 0.19 | 3023 |

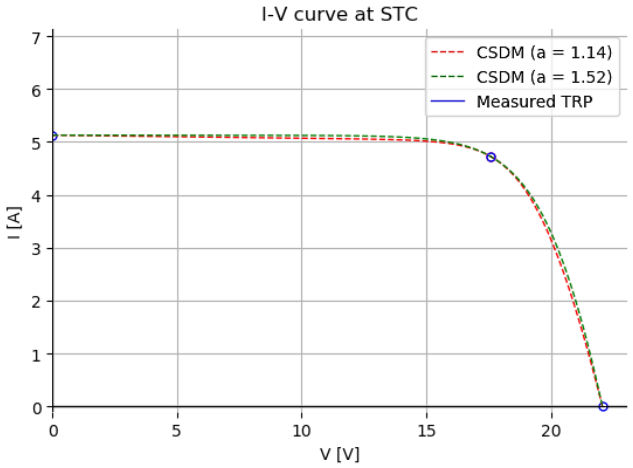


*Figure 8* Modelled I-V curves at STC, the blue dots are the measured TRP

Despite the difference in the RMSD for the two sets is minimal, the differences of the model parameters for the two sets (especially $a$, $R_s$ and $R_p$) are crucial as they have a specific physical meaning: in fact, with respect to the model with $a = 1.14$, the model with $a = 1.52$ inteprets the real PV module as better fabricated in the assembly (lower dissipation through the resistances) but with a poorer semiconductor material (higher ideality factor). This is the fifth piece of information that is missing: in fact, if an I-V dataset at STC was available, the RMSD *on the curve* (i.e. the curve fitting) would have selected the set that best matched the shape of the actual PV device.

In order to evaluate the two sets, the one with $a = 1.52$ is chosen to produce reference values for CPM, while lower values of $a_{max}$ (possibly leading to sets closer to that with $a = 1.14$ at STC) are fed to APM, as for this model the computing time gains importance. This choice will produce results that confirm the insights gained so far.

*Simulations for varying irradiance and temperature*

Figures 12-17 show simulations results for different levels of irradiance and cell temperature. Overall, the models performed excellently.

At high irradiance and temperature (Figure 9), the two models perform almost equally, with an $NRMSD_I$ of 1.24% for APM and 1.82% for CPM. The deviation is registered mainly in the domain of currents, while there is virtually no error on the voltages: if the sensitivity of pyranometers to temperature [23] is considered (the operating temperature is significantly far from the calibration temperature, 20 °C), the results show a quasi-perfect match (Figure 10). A closer look suggests that APM follows better than CPM the shape of the measured curve, meaning that the second best set of parameters at STC (the one with $a = 1.14$, see Table 5) gives a more realistic representation of the actual physics of the real PV module (lower $a$, higher $R_s$, lower $R_p$).

At medium irradiance and temperature (Figure 11), APM shows an NRMSD of 1.02% while CPM scores as high as 2.33%; moreover, CPM shows a -1.8% deviation from $V_{MPP}$: this confirms that the set with $a = 1.14$ is the actual solution. Figure 12 shows the same conditions of irradiance and temperature but with CPM initialized with the correct set at STC: the two models give exactly the same results, i.e. all the errors fall below 0.4% except for $I_{SC}$ (1.8%). However, it is worth noting that, since $I_{SC}$ is lower due to the irradiance, relative higher percentage errors on the currents (and, therefore, on the power) hide absolute errors that are still quite low. For instance, the absolute error on $I_{SC}$ is 0.05 A and a $NRMSD_I$ of 1.02% means $RMSD_I = 0.03\ A$. The absolute error on the $P_{MPP}$ is 0.14 W.

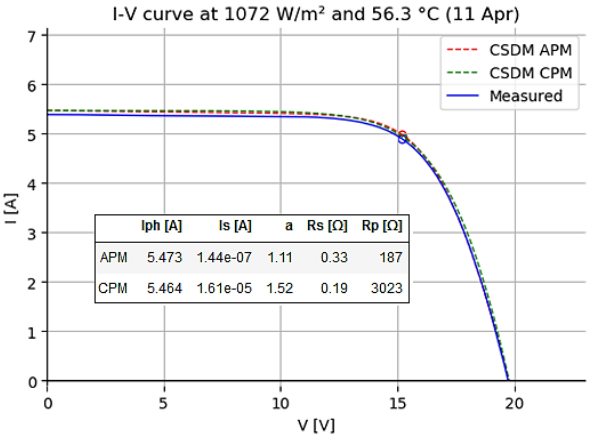


Figure 9 Simulations at high $G$ and high $T_c$

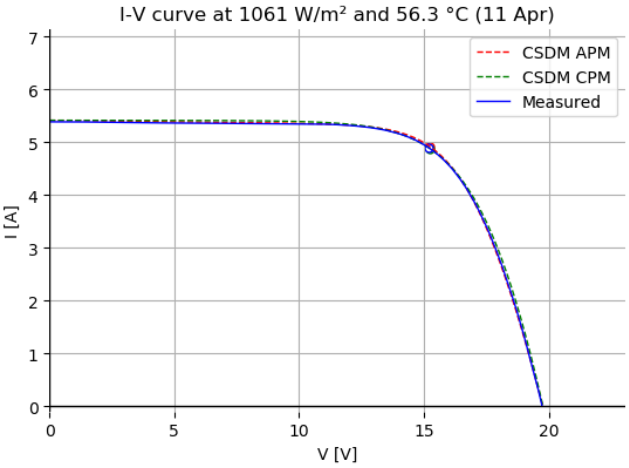


Figure 10 High $G$, high $T_c$ with corrected irradiance

At low irradiance and temperature (Figure 13), both the models are affected by a non-neglectable mismatch, both in the current and voltage domain. This was expected as CSDM is known to perform worse at low irradiance. CPM proves again to have been wrongly-initialized. $NRMSD_I$ is as high as 16.3% for APM and 19.7% for CPM. Errors on the TRP are high on the currents and power (about 21% and 16%, respectively) but lower on the voltages. However, as 11.5°C is fairly far from the calibration temperature of the pyranometer (the sensitivity is more emphasized for

temperatures below the reference [23]), the irradiance can be again adjusted to the lower value in the uncertainty range. Figure 14 shows the effect of this adjustment with the CPM re-initialized with the correct set. Despite the error on $I_{SC}$ is still considerable and the $NRMSD_I$ are still high (about 8%), a significant improvement is registered at the MPP, with CPM now performing slightly better than APM (-0.36% vs 1.48% on $V_{MPP}$). Finally, if a low level of dirtiness is considered, $NRMSD_I$ falls to 2.85% (0.03 A) for APM and 3.79% (0.04 A) for CPM.

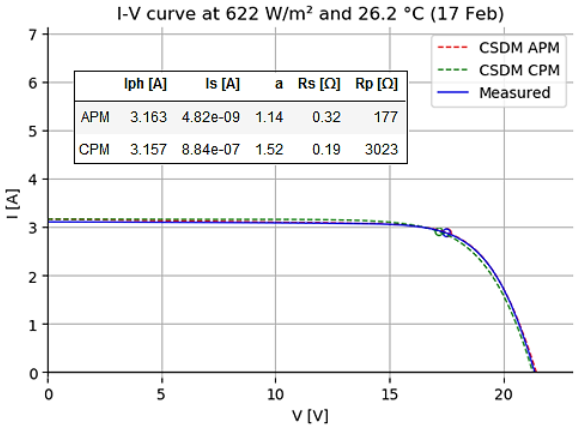


Figure 11 Simulations at medium $G$ and medium $T_c$

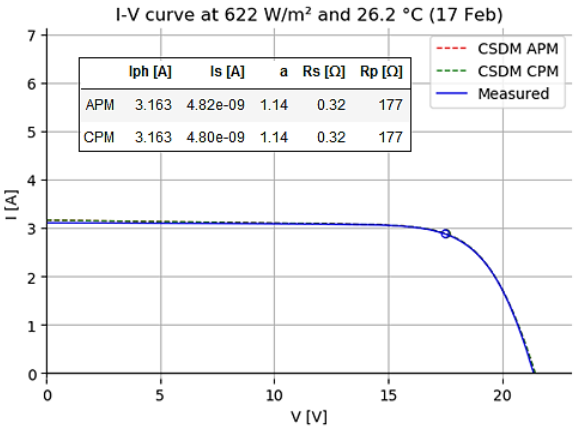


Figure 12 Medium $G$, medium $T_c$ with CPM well-initialized

Also the errors on the MPP drop, with CPM performing better than APM (see Table 6): the high relative error on $I_{SC}$ suggests that a possible source of inaccuracy might be the evaluation of the photocurrent through Equation (12).

APM performed between 265 ms and 600 ms while CPM never took more than 4 ms.

## 7. Conclusions

In this study, a reference framework for PV modelling has been presented and two different Complete Single-Diode Models have been investigated. The preliminary literature review and the built framework showed that different physical approaches and analytical strategies are possible as numerous aspects need to be considered, such as the availability of experimental data.

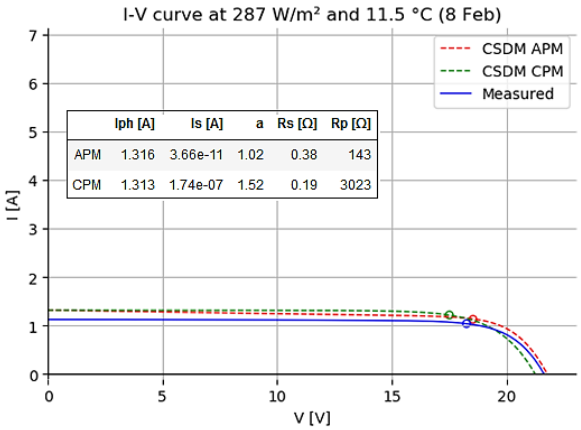


Figure 13 Simulations at low $G$ and low $T_c$

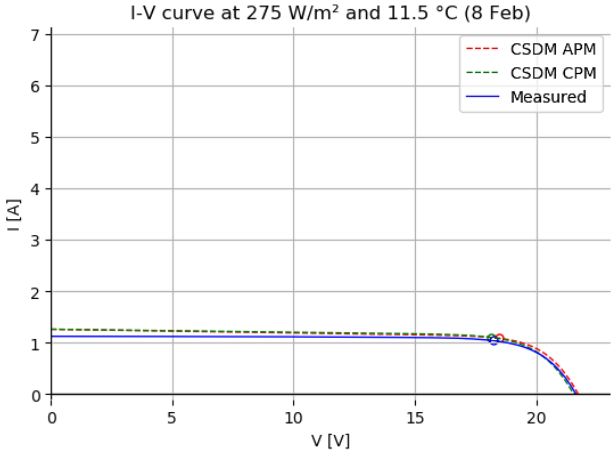


Figure 14 Low $G$, low $T_c$:corrected CPM and adjusted $G$

*Table 6* Errors on corrected CPM (low G, low $T_c$)

| Quantity | Measured | Computed | Absolute Error | Relative Error (%) |
|---|---|---|---|---|
| Isc | 1.1205 | 1.1926 | 0.0721 | 6.44 |
| Voc | 21.6270 | 21.4766 | -0.1504 | -0.70 |
| Pmpp | 18.9362 | 18.7902 | -0.1460 | -0.77 |
| Vmpp | 18.2170 | 18.1229 | -0.0941 | -0.52 |
| Impp | 1.0395 | 1.0368 | -0.0027 | -0.26 |

In the light of these considerations, the 5-parameters model (CSDM) proved to represent the best compromise between simplicity and accuracy. However, since its solving system of equations is dependent, the parameter extraction is affected by a certain level of arbitrariness in the design choices. Therefore, in order to provide additional results for further developments, this model has been implemented according Constant-Parameter Modelling (CPM) and Adaptive-Parameter Modelling (APM).

The analysis of the parameter extraction algorithm based on the matching of the Three Remarkable Points showed that a reasoned design is crucial in terms of accuracy of the results due to the dependent nature of the solving system of equations. In particular, a loop on the ideality factor was set to compensate the missing fifth constraint. However, the width of the range on this loop proved to affect heavily the computing time (crucial for APM) without offering a guaranteed trade-off in terms of

accuracy of the extracted parameters. The simulations showed that the second-best set of parameters modelled more realistically the physics of the tested PV device: by setting a wider range of the loop on the ideality factor, thus supposedly increasing the chances to find the best solution, the actual better set is discarded. Mathematically, this is due to the lack of a *real* fifth physical constraint that brings in information about the shape of the I-V curve.

Both the models proved to match almost perfectly the measured data in any operating condition, showing expected issues at low irradiance. However, these were never too severe and could be justified by taking into account the measurement uncertainties. CPM proved to be sensitive to the preliminary parameter extraction at STC: if it is not conducted properly (e.g. for the abovementioned issue on the shape of the curve) it could cause CPM to mismatch sensibly from reality. However, if CPM is well initialized, it requires hundreds of times less computing time to produce as accurate results as APM (differences lie in the tenth or hundredth per cent). This could be crucial if the model is employed, for instance, in MPPT algorithms or in space applications. Moreover, APM is based on the availability of the temperature coefficients on the current and voltage at MPP, which is not to be taken for granted. Overall, CPM appears to be more rigid and sensitive yet simpler and faster, while APM is more refined but slower and possibly non-implementable.

The good results delivered by the proposed models are based on the previous literature (for instance, the evaluation of the initial guesses for the parameter extraction). Another piece of investigation has been herein conducted providing useful insights about the design of the parameter extraction and the differences between APM and CPM. In this sense, further developments include:

- investigation of a mixed model between the proposed APM and CPM ($I_{ph}$ and $I_s$ are updated while $R_s$ and $R_p$ are extracted with only two constraints, thus avoiding the necessity for temperature coefficients on $I_{MPP}$ and $V_{MPP}$; $a$ is looped),
- a more detailed analysis of the variations of $a$, $R_s$ and $R_p$ with $G$ and $T_c$, with the use of the APM model,
- validation of the proposed models for PV technologies other than monocrystalline silicon,
- extension of the parameter extraction analysis to more complex models such as the Double-Diode Model.

## References


[1] V. Lo Brano, A. Orioli, G. Ciulla e A. Di Gangi, «An improved five-parameter model for photovoltaic modules,» Solar Energy Materials & Solar Cells, vol. 94, n. 8, pp. 1358-1370, 2010.

[2] C. Carrero, J. Amador e S. Arnaltes, «A single procedure for helping PV designers to select silicon PV modules and evaluate the loss resistances,» Renewable Energy, vol. 32, pp. 2579-2589, 2007.

[3] W. Xiao, Photovoltaic Power System: Modeling, Design and Control, John Wiley & Sons, 2017.

[4] A. M. Humada, M. Hojabri, S. Mekhilef e H. M. Hamada, «Solar cell parameters extraction based on single and double-diode model: a review,» Renewable and Sustainable Energy Reviews, n. 56, pp. 494-509, 2016.

[5] M. G. Villalva, J. R. Gazoli e E. R. Filho, «Comprehensive Approach to Modeling and Simulation of Photovoltaic Arrays,» IEEE Transactions on Power Electronics, vol. 25, n. 5, pp. 1198-1208, 2009.

[6] M. N. I. Sarkar, «Effect of various model parameters on solar photovoltaic cell simulation: a SPICE analysis,» Renewables: Wind, Water and Solar, vol. 3, n. 3, 2016.

[7] A. Luque and S. Hegedus, Handbook of Photovoltaic Science and Engineering, John Wiley & Sons, 2011.

[8] A. M. Humada, S. Y. Darweesh, K. G. Mohammed, M. Kamil e et al, «Modeling of PV system and parameter extraction based on experimental data: review and investigation,» Solar Energy, n. 199, pp. 742-760, 2020.

[9] P. Cuce e E. Cuce, «A novel model of photovoltaic modules for parameter estimation and thermodynamic assessment,» International Journal of Low-Carbon Technologies, vol. 7, n. 2, pp. 159-165, 2012.

[10] G. Walker, «Evaluating MPPT converter topologies using a MATLAB PV model,» Journal of Electrical & Electronics Engineering, Vol. %1 di %221-1, pp. 49-56.

[11] A. Kassis e M. Saad, «Analysis of multi-crystalline silicon solar cells at low illumination levels using a modified two-diode model,» Solar Energy Materials and Solar Cells, vol. 94, pp. 2018-2112, 2010.

[12] J. Phang, D. Chan e J. Phillips, «Accurate analytical method for the extraction of solar cell model parameters,» ELectronics Letters, vol. 20, n. 10, pp. 406-408, 1984.

[13] J. Cabestany e X. Castaner, «A simple solar cell series resistance measurement method,» Revue de Physique Appliquée, vol. 18, pp. 565-567, 1983.

[14] E. Matagne, R. Chenni e R. El Bachtiri, «A photovoltaic cell model based on nominal data only,» in CPE-POWERENG, Setubal (PT), 2007.

[15] V. Lo Brano e G. Ciulla, «An efficient analytical approach for obtaining a five parameters model of photovoltaic modules using only reference data,» Applied Energy, n. 111, pp. 894-903, 2013.

[16] D. S. H. Chan e J. C. H. Phang, «Analytical Methods for the Extraction of Solar-Cell Single- and Double-Diode Model Parameters from I-V Characteristics,» IEEE Transactions on Electron Devices, vol. 34, n. 2, 1987.

[17] W. De Soto, S. Klein e W. Beckman, «Improvement and validation of a model for photovoltaic array performance,» Solar Energy, n. 80, pp. 78-88, 2006.

[18] W. Xiao, W. G. Dunford e A. Capel, «A Novel Modeling Method for Photovoltaic Cells,» in 35th Annual IEEE Power Electronics Specialists Conference, Aachen, Germany, 2004.

[19] K. Ishaque, Z. Salam e H. Taheri, «Simple, fast and accurate two-diode model for photovoltaic modules,» Solar Energy Materials & Solar Cells, n. 95, pp. 586-594, 2011.

[20] J. Gow e C. Manning, «Development of a photovoltaic array model for use in power-electronics simulation studies,» IEE Proceedings - Electric Power Applications , vol. 146, n. 2, pp. 193-200, 1999.

[21] K. Nishioka, N. Sakitani, Y. Uraoka e T. Fuyuki, «Analysis of multicristalline silicon solar cells by modified 3-diode equivalent circuit model taking leakage current through periphery into consideration,» Solar Energy Materials and Solar Cells, vol. 91, pp. 1222-1227, 2007.

[22] W. Marion, A. Anderberg, C. Deline e et al., «User's Manual for Data for Validating Models for PV Module Performance,» NREL, April 2014. [Online]. Available: https://www.nrel.gov/docs/fy14osti/61610.pdf.

[23] M. Korevaar, «The Importance of Pyranometer Temperature Response,» Kipp&Zonen, 9 March 2015. [Online]. Available: https://www.kippzonen.com/News/582/The-Importance-of-Pyranometer-Temperature-Response.